

Coupled-channel interpretation of the LHCb double- J/ψ spectrum and hints of a new state near $J/\psi J/\psi$ threshold

Xiang-Kun Dong,^{1, 2} Vadim Baru,^{3, 4, 5} Feng-Kun Guo,^{1, 2} Christoph Hanhart,⁶ and Alexey Nefediev^{5, 7, 8}

¹*CAS Key Laboratory of Theoretical Physics, Institute of Theoretical Physics, Chinese Academy of Sciences, Zhong Guan Cun East Street 55, Beijing 100190, China*

²*School of Physical Sciences, University of Chinese Academy of Sciences, Beijing 100049, China*

³*Helmholtz-Institut für Strahlen- und Kernphysik and Bethe Center for Theoretical Physics, Universität Bonn, D-53115 Bonn, Germany*

⁴*Institute for Theoretical and Experimental Physics NRC “Kurchatov Institute”, Moscow 117218, Russia*

⁵*P.N. Lebedev Physical Institute of the Russian Academy of Sciences, 119991, Leninskiy Prospect 53, Moscow, Russia*

⁶*Institute for Advanced Simulation, Institut für Kernphysik and Jülich Center for Hadron Physics, Forschungszentrum Jülich, D-52425 Jülich, Germany*

⁷*Moscow Institute of Physics and Technology, 141700, Institutsky lane 9, Dolgoprudny, Moscow Region, Russia*

⁸*National Research Nuclear University MEPhI, 115409, Kashirskoe highway 31, Moscow, Russia*

Recently, the LHCb Collaboration reported pronounced structures in the invariant mass spectrum of J/ψ -pairs produced in proton-proton collisions at the Large Hadron Collider. In this Letter, we argue that the data can be very well described within two variants of a unitary coupled-channel approach: (i) with just two channels, $J/\psi J/\psi$ and $\psi(2S)J/\psi$, as long as energy-dependent interactions in these channels are allowed, or (ii) with three channels $J/\psi J/\psi$, $\psi(2S)J/\psi$ and $\psi(3770)J/\psi$ with just constant contact interactions. Both formulations hint at the existence of a near-threshold state in the $J/\psi J/\psi$ system with the quantum numbers $J^{PC} = 0^{++}$ or 2^{++} , which we refer to as $X(6200)$. We suggest experimental tests to check the existence of this state and discuss what additional channels need to be studied experimentally to allow for distinctive tests between the two mechanisms proposed. If the molecular nature of the $X(6200)$, as hinted by the three-channel approach, were confirmed, many other double-quarkonium states should exist driven by the same binding mechanisms.

INTRODUCTION

Quantum chromodynamics (QCD) as the fundamental theory for the strong interaction is highly nonperturbative at low energies. As a result, how the hadrons emerge from QCD and how the hadron spectrum is organized are still challenging open questions. The quest of exotic hadrons beyond the conventional quark model classification of quark-antiquark mesons and three-quark baryons has been one of the central issues in the study of non-perturbative QCD. In the past decades, dozens of new resonant structures with exotic properties were reported by various experiments in particular in the spectrum of hadrons containing at least one heavy-flavor (charm or bottom) quark. However, these observations brought even more challenges as they seem not to fit into a single uniform classification scheme, and various interpretations were proposed for each of them, see Refs. [1–9] for recent reviews of such exotic states.

Recently, the LHCb Collaboration reported resonant structures in the double- J/ψ invariant mass distribution using data for pp collisions at the c.m. energies 7, 8 and 13 TeV [10]. The form of the signal reported by LHCb in the invariant mass region from 6.2 ($J/\psi J/\psi$ threshold) to approximately 7.2 GeV is quite nontrivial, departing significantly from the expected trivial phase space as well as the single and double-parton scattering. In particular, an enhancement in the near-double- J/ψ threshold region from 6.2 to 6.8 GeV is seen, which is

followed by a narrow peak around 6.9 GeV. Between the broad bump and the narrow peak, there is a dip around 6.8 GeV. The narrow peak is now dubbed $X(6900)$, and has spurred a flood of model explanations [11–27]. Naturally, a fully-charm compact tetraquark resonance is the most straightforward candidate. However, most of the theoretical studies indicate that the $cc\bar{c}\bar{c}$ ground state should have a mass lower than 6.9 GeV [28–35]. Furthermore, the 700 MeV energy gap between the double- J/ψ threshold and 6.9 GeV is larger than a typical energy gap between the ground and radially/orbitally excited states. Thus a natural expectation would be that lower states should exist, if there is a $cc\bar{c}\bar{c}$ resonance with a mass around 6.9 GeV. Due to a smaller phase space, such lighter states are expected to have smaller widths. However, there are no obvious narrower peaks in the reported double- J/ψ spectrum.

It is well-known that threshold effects play an important, sometimes crucial, role for the properties of hadrons residing above the open-flavor threshold. For example, there is always a cusp at an S -wave threshold due to the analytic structure of the two-body Green’s function (for a recent review of the threshold effects related to the exotic hadrons, we refer to [8]). It may lead to either a peak or a dip, depending on the interference with other contributions. The visibility of the corresponding structure in the line shape depends on whether or not it is enhanced by a nearby pole in the amplitude [36]. Thus, in order to properly interpret the new observations it is important

to understand the role played by various thresholds located nearby. There are quite a few double-charmonium channels with thresholds below 7.2 GeV that can couple to the double- J/ψ system, such as $\eta_c\eta_c$, $h_c h_c$, $\chi_{cJ}\chi_{cJ'}$ ($J, J' = 0, 1, 2$), $\psi(2S)J/\psi$ and $\psi(3770)J/\psi$. Among these channels, the coupling of the double- J/ψ to the $\eta_c\eta_c$ or $h_c h_c$ flips the charm-quark spin, and is expected to be suppressed due to the heavy quark spin symmetry (HQSS). From the point of view of the meson-exchange picture, the lowest meson that can be exchanged, while keeping the SU(3) flavor and isospin symmetries, for the coupling of the $\chi_{cJ}\chi_{cJ'}$ to the double- J/ψ is the ω . It is heavier than the $f_0(500)$ (or effectively two pions) that can be exchanged for $J/\psi J/\psi \rightarrow \psi(2S)J/\psi$ or $\psi(3770)J/\psi$ to happen. In this regard, it is interesting to notice that indeed the dip prior to the $X(6900)$ peak appears around the $\psi(2S)J/\psi$ threshold at 6783 MeV. Therefore, from this phenomenological point of view, among the double-charmonium channels, the $\psi(2S)J/\psi$ and $\psi(3770)J/\psi$ ones are expected to play the most crucial role in describing the double- J/ψ spectrum up to an energy covering the $X(6900)$ peak.

In this Letter, we aim at constructing minimal coupled-channel models able to describe the LHCb data on the double- J/ψ invariant mass distribution in the energy interval from double- J/ψ threshold to 7.2 GeV and studying their predictions for pole locations and line shapes in the other double-charmonium channels. In particular, we consider a two-channel ($J/\psi J/\psi$ and $\psi(2S)J/\psi$) and a three-channel ($J/\psi J/\psi$, $\psi(2S)J/\psi$, and $\psi(3770)J/\psi$) model and find that (i) both models provide a remarkably good description of the data which, therefore, do not allow one to distinguish between them, (ii) both models predict the existence of a near-threshold pole around 6.2 GeV (we call it the $X(6200)$) corresponding to a shallow bound or virtual $J/\psi J/\psi$ state, (iii) the structure of the other, above-threshold poles appears to be very different for the two models considered and so are the predicted line shapes in the $\psi(2S)J/\psi$ channel. We conclude, therefore, that the existence of the $X(6200)$ is a robust consequence of the proposed coupled-channel approach, while additional measurements of the other double-charmonium channels are necessary in order to better understand the nature of the higher poles.

THE COUPLED-CHANNEL MODEL

Contrary to earlier attempts to understand the role played by the relevant double-charmonium thresholds for the double- J/ψ spectrum [23], the key idea of our approach is to present a minimal model consistent with the data and able to extract the positions of the poles responsible for the structures in the line shape from the data. We, therefore, confine ourselves to those double-charmonium channels which are consistent with

the HQSS, and constrain the amplitude with unitarity and causality. Thus, we focus on two variants of the coupled-channel model, a two-channel model employing $\{J/\psi J/\psi, \psi(2S)J/\psi\}$ and a three-channel model using $\{J/\psi J/\psi, \psi(2S)J/\psi, \psi(3770)J/\psi\}$.

As detailed below we work with a separable potential V . Then the T -matrix of the coupled-channel system can be written as

$$T(E) = V(E) \cdot [1 - G(E)V(E)]^{-1}, \quad (1)$$

where E is the double- J/ψ center-of-mass energy and G is a diagonal matrix for the intermediate two-body propagators. We use the dimensionally regularized two-point scalar loop function [37],

$$G_i(E) = \frac{1}{16\pi^2} \left\{ a(\mu) + \log \frac{m_{i1}^2}{\mu^2} + \frac{m_{i2}^2 - m_{i1}^2 + s}{2s} \log \frac{m_{i2}^2}{m_{i1}^2} \right. \\ \left. + \frac{k_i}{E} \log \frac{(2k_i E + s)^2 - m_{i1}^2 + m_{i2}^2}{(2k_i E - s)^2 - m_{i1}^2 + m_{i2}^2} \right\}, \quad (2)$$

where $s = E^2$, m_{i1} and m_{i2} are the particle masses in the i -th channel, $k_i = \lambda^{1/2}(E^2, m_{i1}^2, m_{i2}^2)/(2E)$ is the corresponding three-momentum with $\lambda(x, y, z) = x^2 + y^2 + z^2 - 2xy - 2yz - 2xz$ for the Källén triangle function. Here μ denotes the dimensional regularization scale, and $a(\mu)$ is a subtraction constant. The T -matrix provided in Eq. (1) is unitary by construction.

For the two-channel model the 2×2 matrix of the potential V is parameterized as

$$V_{2\text{ch}}(E) = \begin{pmatrix} a_1 + b_1 k_1^2 & c \\ c & a_2 + b_2 k_2^2 \end{pmatrix}, \quad (3)$$

where $a_{1,2}$, $b_{1,2}$, and c are real free parameters. The energy dependence of the potential is necessary here to be able to produce nontrivial structures above the higher threshold, since purely constant contact-term potential can only produce bound or virtual state poles below threshold.

For the three-channel model the potential V is a 3×3 matrix,

$$V_{3\text{ch}}(E) = \begin{pmatrix} a_{11} & a_{12} & a_{13} \\ a_{12} & a_{22} & a_{23} \\ a_{13} & a_{23} & a_{33} \end{pmatrix}, \quad (4)$$

where a_{ij} 's are real parameters of the model, and no explicit dependence of the potential on the energy is necessary given that the uppermost threshold in this variant of the model lies above the structures in the mass spectrum.

The production amplitude in the $J/\psi J/\psi$ channel (labelled as channel 1) can be constructed as

$$\mathcal{M}_1 = P(E) \left[1 + \sum_i r_i G_i(E) T_{i1}(E) \right], \quad (5)$$

where T_{ij} are the elements of the T -matrix in Eq. (1), the unity inside the square brackets describes the contribution of the coherent background and the ratios r_i mimic slightly different production mechanisms for different channels. To describe the details of the short-distance production encoded in the function $P(E)$ above we take it in an exponential form,

$$P(E) = \alpha e^{-\beta E^2}, \quad (6)$$

and fix the slope parameter $\beta = 0.0123 \text{ GeV}^{-2}$ from fitting to the double-parton scattering (DPS) distribution quoted in the LHCb paper [10]. The energy dependence of the production operator accounts for the fact that the double- J/ψ and $\psi(2S)J/\psi$ two-particle systems can be produced at the parton level and interact before the final double- J/ψ particles are detected. The overall strength parameter α is treated as yet another free parameter of the model.

Finally, the experimental double- J/ψ distribution is fitted with the function $\rho(E)|\mathcal{M}_1|^2$, where $\rho(E) = k_1/(8\pi E)$ is the double- J/ψ phase space factor.

FIT RESULTS

Before we come to fitting the data let us get rid of the parameters which weakly affect the distribution or can be recast into other constants. In particular, we set $\mu = 1 \text{ GeV}$ and the subtraction constant in the loop function is fixed as $a(\mu = 1 \text{ GeV}) = -3$; its variance can be absorbed into the redefinition of the contact interactions in the potential. Also, we choose all r -parameters in the amplitude (5) equal for the fit did not call for different values.

Two-channel model: The two-channel parameterization has 7 parameters. These are $\{a_1, a_2, b_1, b_2, c, r, \alpha\}$. The fit was performed with randomly chosen 2×10^4 sets of initial values of the parameters, and constrained by causality which requires that there should be no pole on the first Riemann sheet of the complex energy except on the real axis below threshold (see, e.g., Ref. [38]). More than 20 fits were found with $\chi^2/\text{dof} < 1.25$. However, only one fit survives after removing those having narrow spikes in the spectrum (with a width smaller than 28 MeV, the size of the energy bin in the data). The best fit describes the data remarkably well with $\chi^2/\text{dof} = 0.99$, see Fig. 1. Interestingly, although the fit was only performed up to 7.2 GeV, a good description of the data is achieved in the entire energy interval up to 9 GeV. In this model, the dip in the line shape is produced due to a destructive interference of the $\psi(2S)J/\psi$ threshold cusp which emerges from a coupled-channel dynamics with the background. The above-threshold narrow hump is due to the energy dependence of the two-channel potential (3) which leads to a nearby resonance pole. A detailed analysis of the poles is given later.

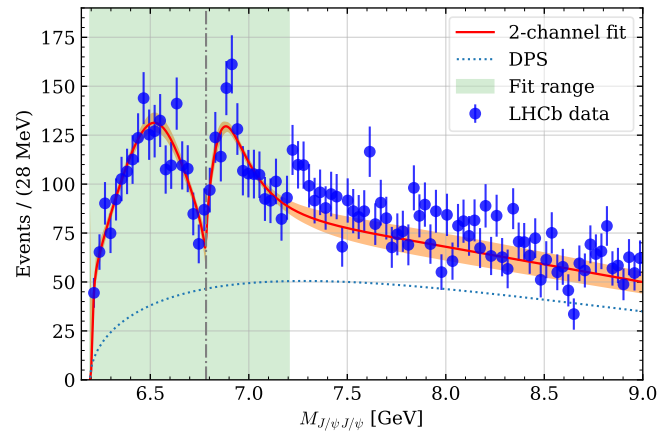


FIG. 1. Two-channel fit to the LHCb data of the double- J/ψ invariant mass distribution [10]. The solid line is the best fit with $\chi^2/\text{dof} = 0.99$, and the band is the 1σ error area. The dotted line denotes $P(E)$ in Eq. (6) which describes perfectly the DPS distribution taken from the LHCb analysis [10] to fix parameter β in Eq. (6). The $\psi(2S)J/\psi$ threshold is shown as the vertical dash-dotted line.

Three-channel model: The three-channel model has 8 real parameters, $\{a_{ij} (i \geq j), r, \alpha\}$. Two fits of similar quality can be found which have $\chi^2/\text{dof} = 0.97$ (Fit 1) and $\chi^2/\text{dof} = 1.05$ (Fit 2). All parameters of these fits coincide within their 1σ uncertainty except a_{22} . A comparison of both fits with the data is given in Fig. 2. Like in the two-channel model, the description of the data is remarkably good, including the (not fitted) large-energy tail up to 9 GeV. In this model, the nontrivial structures in the line shape at approximately 6.8 and 6.9 GeV are due to the effect from the $\psi(2S)J/\psi$ and $\psi(3770)J/\psi$ thresholds, amplified by a nearby pole.

POLE ANALYSIS

We are now in the position to study the pole structure of the amplitudes which emerges from fitting the two- and three-channel models described above. To this end, we generate more than 300 parameter sets within the 1σ contours in the parameter space for all combinations of the fit parameters and find all poles of the amplitude in the near-threshold region from 6.2 to 7.2 GeV. The results are presented in Figs. 3 and 4 from which one can draw several conclusions.

We focus first on the mass region of the pronounced structures in the data. Here the location of the poles is quite different for the different models: while there is only one pole for the three-channel models, there exist two such poles for the two-channel model. They are (in

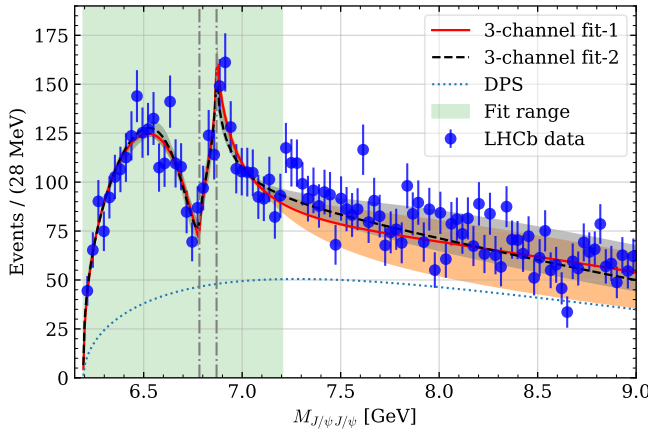


FIG. 2. Three-channel fits to the LHCb data [10] of the double- J/ψ invariant mass distribution. Fit 1 with $\chi^2/\text{dof} = 0.97$ and Fit 2 with $\chi^2/\text{dof} = 1.05$ are shown as the solid and dashed curves, respectively, together with the corresponding 1σ error bands. The dotted line is defined the same as in Fig.1. The $\psi(2S)J/\psi$ and $\psi(3770)J/\psi$ thresholds are shown as the vertical dash-dotted lines.

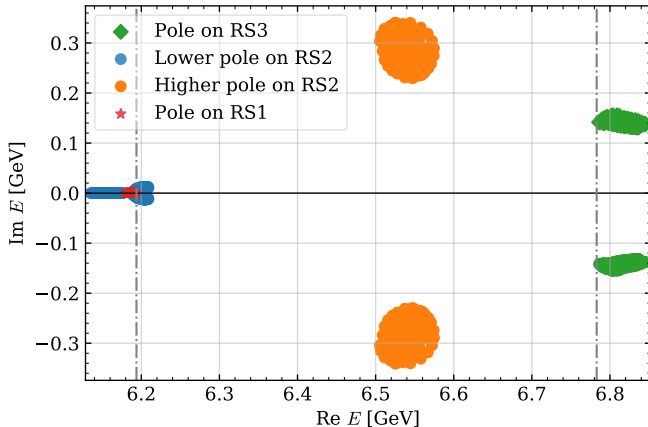


FIG. 3. Poles of the T -matrix from the 2-channel fit.

units of MeV; the same for the following results)

$$\begin{aligned} E_1^{2\text{ch}} &= 6542^{+33}_{-36} - i 282^{+59}_{-52} \text{ (RS2)}, \\ E_2^{2\text{ch}} &= 6818^{+28}_{-32} - i 142^{+14}_{-10} \text{ (RS3)}, \end{aligned} \quad (7)$$

for the two-channel model, where RS1, RS2 and RS3 quoted in parentheses refer to the first, second and third Riemann sheets. There is a single pole on RS2 for the 3-channel fits, which, however, is far from the physical region with a badly located pole position, see Fig. 4.

Meanwhile, both models predict a pole very near the $J/\psi J/\psi$ threshold. The two-channel fit allows for a bound-state, a virtual-state or a resonance pole,

$$E_0^{2\text{ch}} = 6203^{+6}_{-27} - i 12^{+1}_{-12} \text{ (RS2) or } [6179, 6194] \text{ (RS1).} \quad (8)$$

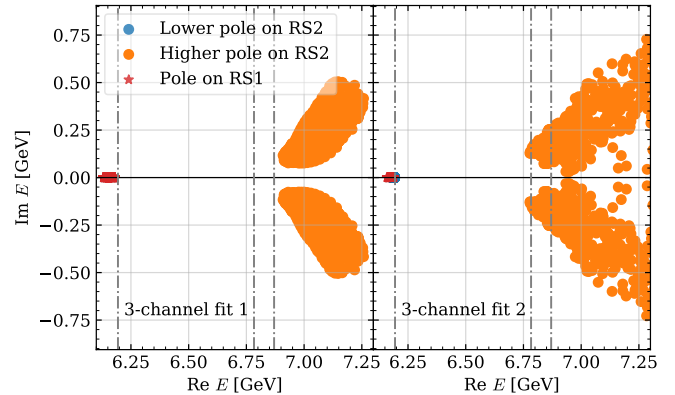


FIG. 4. Poles of the T -matrix from the 3-channel fits.

The two best three-channel fits give

$$\begin{aligned} E_0^{3\text{ch}}[\text{Fit 1}] &= 6163^{+18}_{-32} \text{ (RS1),} \\ E_0^{3\text{ch}}[\text{Fit 2}] &= 6189^{+5}_{-10} \text{ (RS2) or } [6159, 6194] \text{ (RS1).} \end{aligned} \quad (9)$$

Thus, the pole for Fit 1 represents a bound state, while for Fit 2 it can be either a shallow bound or virtual state.

Obviously, further modifications of the model to extend the coupled-channel set or to include higher-order terms in the potential cannot destroy this pole simply because such modifications would only affect the high-energy tail of the distribution, far away from the $J/\psi J/\psi$ near-threshold region. We conclude, therefore, that the existence of a pole near the $J/\psi J/\psi$ threshold is a robust consequence of the coupled-channel dynamics within the suggested approach. For definiteness, we name this state $X(6200)$. The quantum numbers of this state are either 0^{++} or 2^{++} , as required to have an S -wave threshold composed by two identical vector bosons.

FURTHER PREDICTIONS AND TESTS

As one can see from Figs. 1 and 2, although the models used to analyse the data in the $J/\psi J/\psi$ channel are based on a different dynamical content, they can provide a description of the data of a comparable quality. However, further predictions of these models differ substantially, allowing for a direct experimental discrimination (or falsification of the whole approach). As one of such tests we propose measurements of the line shapes in the other double-charmonium channels. As a representative example, in Fig. 5 we show the predictions of the two models employed in this work for the invariant mass spectrum in the $\psi(2S)J/\psi$ final state. Indeed, the models provide quite different spectra above the $\psi(3770)J/\psi$ threshold, so that experimental data for this channel as well as for the $\psi(3770)J/\psi$ should help to better understand the physical origin of the structures reported by LHCb.

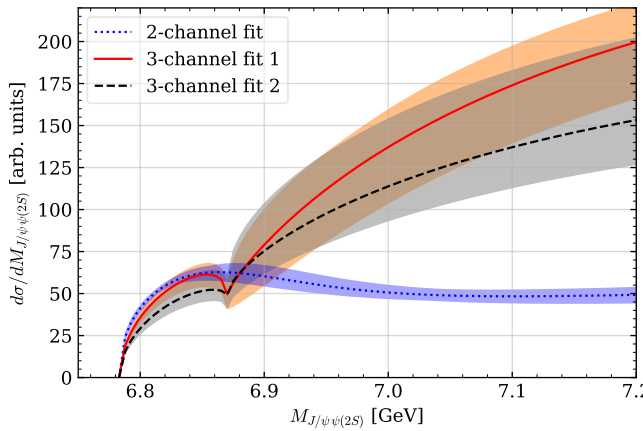


FIG. 5. Predictions for the invariant mass spectrum in the $\psi(2S)J/\psi$ final state.

Also, a direct experimental confirmation or refutation of the existence of the $X(6200)$ state is very important for a better understanding of the double-charmonium spectrum. In particular, a clear signal from this state could be seen in the final states $J/\psi\mu^+\mu^-$ and $\mu^+\mu^+\mu^-\mu^-$ which can be studied at energies below the nominal $J/\psi J/\psi$ threshold.

To better understand the nature of the $X(6200)$, we estimate its compositeness, \bar{X}_A following Ref. [39]. To this end, we employ the effective range expansion of the scattering amplitude in the $J/\psi J/\psi$ channel,

$$T(k) = -8\pi\sqrt{s} \left[\frac{1}{a} + \frac{1}{2}rk^2 - ik + \mathcal{O}(k^4) \right]^{-1}, \quad (10)$$

to extract the scattering length a and the effective range r , and then use

$$\bar{X}_A = (1 + 2|r/a|)^{-1/2}. \quad (11)$$

The results presented in Table I imply that while the two-channel model supports the $X(6200)$ as a compact state, the three-channel approach is compatible with its molecular interpretation. If the latter is true, same mechanisms which drive the $X(6200)$ can provide sufficient binding also in other double-charmonium channels, so that many more double-charmonium molecular states can exist near relevant thresholds.

CONCLUSION

In this Letter, we have demonstrated that the recent LHCb data on the invariant mass spectrum in the $pp \rightarrow J/\psi J/\psi$ reaction are consistent with a coupled-channel description. The best fits of the model to the data implies the existence of a state near the $J/\psi J/\psi$ threshold which we called the $X(6200)$. This state can have the quantum numbers of a scalar or a tensor. Further experimental

TABLE I. The effective range parameters in the $J/\psi J/\psi$ channel and the compositeness \bar{X}_A of the $X(6200)$. Please note that in some cases the uncertainty in the pole position of the $X(6200)$ does not allow one to extract the sign of the scattering length which by convention is negative (positive) if the $X(6200)$ is a bound (virtual) state.

	2-ch. fit	3-ch. fit 1	3-ch. fit 2
$a(\text{fm})$	$\leq -0.49 \text{ or } \geq 0.48$	$-0.61^{+0.29}_{-0.32}$	$\leq -0.60 \text{ or } \geq 0.99$
$r(\text{fm})$	$-2.18^{+0.66}_{-0.81}$	$-0.06^{+0.03}_{-0.04}$	$-0.09^{+0.08}_{-0.05}$
\bar{X}_A	$0.39^{+0.58}_{-0.12}$	$0.91^{+0.04}_{-0.07}$	$0.95^{+0.04}_{-0.06}$

tests are outlined to test the hypothesis of the existence of this state and to shed light on its nature. If confirmed, this discovery may start a new era in the spectroscopy of double-charmonium and double-bottomonium states.

This work is supported in part by the National Natural Science Foundation of China (NSFC) under Grants No. 11835015, No. 11961141012 and No. 11947302, by the NSFC and the Deutsche Forschungsgemeinschaft (DFG) through the funds provided to the Sino-German Collaborative Research Center “Symmetries and the Emergence of Structure in QCD” (NSFC Grant No. 11621131001, DFG Grant No. CRC110), by the Chinese Academy of Sciences (CAS) under Grants No. XDB34030303 and No. QYZDB-SSW-SYS013, and by the CAS Center for Excellence in Particle Physics (CCEPP). Work of V.B. and A.N. was supported by the Russian Science Foundation (Grant No. 18-12-00226).

Appendix: Values of the T -matrix parameters

Here we give the values of the T -matrix parameters and their correlation matrices from the fits discussed in the main text.

For the two-channel fit, the parameter values are

$$a_1 = 0.2^{+0.6}_{-0.5}, \quad a_2 = -4.2 \pm 0.7, \quad c = 2.94^{+0.36}_{-0.29}, \\ b_1 = -1.8^{+0.4}_{-0.5} \text{ GeV}^{-2}, \quad b_2 = -7.1 \pm 0.4 \text{ GeV}^{-2}. \quad (12)$$

The correlation matrix is given by

$$\begin{pmatrix} 1 & 0.33 & 0.25 & -0.82 & 0.24 \\ 0.33 & 1 & -0.04 & -0.45 & 0.97 \\ 0.25 & -0.04 & 1 & -0.50 & -0.21 \\ -0.82 & -0.45 & -0.50 & 1 & -0.35 \\ 0.24 & 0.97 & -0.21 & -0.35 & 1 \end{pmatrix}. \quad (13)$$

For the three-channel Fit 1, the parameter values are

$$a_{11} = 6.0^{+2.2}_{-1.6}, \quad a_{12} = 10.3^{+3.4}_{-2.8}, \quad a_{13} = -0.2^{+1.9}_{-1.3}, \\ a_{22} = 13^{+5}_{-4}, \quad a_{23} = -120^{+110}_{-60}, \quad a_{33} = -2.3^{+1.5}_{-1.1}. \quad (14)$$

The correlation matrix is given by

$$\begin{pmatrix} 1 & 0.94 & 0.57 & 0.82 & 0.56 & -0.38 \\ 0.94 & 1 & 0.74 & 0.93 & 0.70 & -0.52 \\ 0.57 & 0.74 & 1 & 0.92 & 0.98 & -0.93 \\ 0.82 & 0.93 & 0.92 & 1 & 0.90 & -0.78 \\ 0.56 & 0.70 & 0.98 & 0.90 & 1 & -0.94 \\ -0.38 & -0.52 & -0.93 & -0.78 & -0.94 & 1 \end{pmatrix}. \quad (15)$$

For the three-channel Fit 2, the parameter values are

$$\begin{aligned} a_{11} &= 7.8_{-2.0}^{+3.4}, \quad a_{12} = 16 \pm 4, \quad a_{13} = 0.9_{-2.5}^{+2.3}, \\ a_{22} &= 26_{-6}^{+12}, \quad a_{23} = -120_{-210}^{+190}, \quad a_{33} = -2.5_{-1.0}^{+2.1}. \end{aligned} \quad (16)$$

The correlation matrix is given by

$$\begin{pmatrix} 1 & 0.80 & 0.08 & 0.64 & 0.01 & 0.09 \\ 0.80 & 1 & 0.03 & 0.96 & -0.07 & 0.24 \\ 0.08 & 0.03 & 1 & 0.14 & 0.98 & -0.91 \\ 0.64 & 0.96 & 0.14 & 1 & 0.04 & 0.15 \\ 0.01 & -0.07 & 0.98 & 0.04 & 1 & -0.92 \\ 0.09 & 0.24 & -0.91 & 0.15 & -0.92 & 1 \end{pmatrix}. \quad (17)$$

[1] A. Hosaka, T. Iijima, K. Miyabayashi, Y. Sakai and S. Yasui, PTEP **2016**, 062C01 (2016) [arXiv:1603.09229 [hep-ph]].

[2] R. F. Lebed, R. E. Mitchell and E. S. Swanson, Prog. Part. Nucl. Phys. **93**, 143-194 (2017) [arXiv:1610.04528 [hep-ph]].

[3] A. Esposito, A. Pilloni and A. D. Polosa, Phys. Rept. **668**, 1-97 (2017) [arXiv:1611.07920 [hep-ph]].

[4] F.-K. Guo, C. Hanhart, U.-G. Meißner, Q. Wang, Q. Zhao and B.-S. Zou, Rev. Mod. Phys. **90**, 015004 (2018) [arXiv:1705.00141 [hep-ph]].

[5] S. L. Olsen, T. Skwarnicki and D. Zieminska, Rev. Mod. Phys. **90**, 015003 (2018) [arXiv:1708.04012 [hep-ph]].

[6] Y.-R. Liu, H.-X. Chen, W. Chen, X. Liu and S.-L. Zhu, Prog. Part. Nucl. Phys. **107**, 237-320 (2019) [arXiv:1903.11976 [hep-ph]].

[7] N. Brambilla, S. Eidelman, C. Hanhart, A. Nefediev, C.-P. Shen, C. E. Thomas, A. Vairo and C.-Z. Yuan, Phys. Rept. **873**, 1 (2020) [arXiv:1907.07583 [hep-ex]].

[8] F.-K. Guo, X.-H. Liu and S. Sakai, Prog. Part. Nucl. Phys. **112**, 103757 (2020) [arXiv:1912.07030 [hep-ph]].

[9] G. Yang, J. Ping and J. Segovia, [arXiv:2009.00238 [hep-ph]].

[10] R. Aaij *et al.* [LHCb Collaboration], arXiv:2006.16957 [hep-ex].

[11] M. S. Liu, F. X. Liu, X. H. Zhong and Q. Zhao, arXiv:2006.11952 [hep-ph].

[12] Z. G. Wang, arXiv:2006.13028 [hep-ph].

[13] X. Jin, Y. Xue, H. Huang and J. Ping, arXiv:2006.13745 [hep-ph].

[14] G. Yang, J. Ping, L. He and Q. Wang, arXiv:2006.13756 [hep-ph].

[15] Q. F. L, D. Y. Chen and Y. B. Dong, arXiv:2006.14445 [hep-ph].

[16] H. X. Chen, W. Chen, X. Liu and S. L. Zhu, arXiv:2006.16027 [hep-ph].

[17] X. Y. Wang, Q. Y. Lin, H. Xu, Y. P. Xie, Y. Huang and X. Chen, arXiv:2007.09697 [hep-ph].

[18] J. Sonnenschein and D. Weissman, arXiv:2008.01095 [hep-ph].

[19] R. M. Albuquerque, S. Narison, A. Rabemananjara, D. Rabetiarivony and G. Randriamananjara, arXiv:2008.01569 [hep-ph].

[20] J. F. Giron and R. F. Lebed, arXiv:2008.01631 [hep-ph].

[21] L. Maiani, arXiv:2008.01637 [hep-ph].

[22] J. M. Richard, arXiv:2008.01962 [hep-ph].

[23] J. Z. Wang, D. Y. Chen, X. Liu and T. Matsuki, arXiv:2008.07430 [hep-ph].

[24] K. T. Chao and S. L. Zhu, Science Bulletin (2020)

[25] R. Maciua, W. Schäfer and A. Szczurek, arXiv:2009.02100 [hep-ph].

[26] M. Karliner and J. L. Rosner, arXiv:2009.04429 [hep-ph].

[27] Z. G. Wang, arXiv:2009.05371 [hep-ph].

[28] J. P. Ader, J. M. Richard and P. Taxil, Phys. Rev. D **25**, 2370 (1982)

[29] A. M. Badalian, B. L. Ioffe and A. V. Smilga, Nucl. Phys. B **281**, 85 (1987)

[30] J. Wu, Y. R. Liu, K. Chen, X. Liu and S. L. Zhu, Phys. Rev. D **97**, 094015 (2018) [arXiv:1605.01134 [hep-ph]].

[31] M. Karliner, S. Nussinov and J. L. Rosner, Phys. Rev. D **95**, 034011 (2017) [arXiv:1611.00348 [hep-ph]].

[32] Z. G. Wang, Eur. Phys. J. C **77**, 432 (2017) [arXiv:1701.04285 [hep-ph]].

[33] M. S. Liu, Q. F. L, X. H. Zhong and Q. Zhao, Phys. Rev. D **100**, 016006 (2019) [arXiv:1901.02564 [hep-ph]].

[34] M. A. Bedolla, J. Ferretti, C. D. Roberts and E. Santopinto, [arXiv:1911.00960 [hep-ph]].

[35] X. Chen, [arXiv:2001.06755 [hep-ph]].

[36] F.-K. Guo, C. Hanhart, Q. Wang and Q. Zhao, Phys. Rev. D **91**, 051504 (2015)

[37] M. J. G. Veltman, Cambridge Lect. Notes Phys. **4**, 1 (1994)

[38] V. N. Gribov, Y. L. Dokshitzer and J. Nyiri, Camb. Monogr. Part. Phys. Nucl. Phys. Cosmol. **27** (2012)

[39] I. Matuschek, V. Baru, F.-K. Guo and C. Hanhart, arXiv:2007.05329 [hep-ph].